Essential Readings in Light Metals: Cast Shop for Aluminum Production.
Edited by John F. Grandfield and Dmitry G. Eskin.

A RADIOSCOPIC TECHNIQUE TO OBSERVE BUBBLES IN LIQUID ALUMINUM

Marc Bertherat*†, Thierry Odièvre**, Michel Allibert*, Pierre Le Brun**

*INP Grenoble, Laboratoire de Thermodynamique et Physico Chimie Métallurgiques,
ENSEEG BP75 38402 St Martin d'Hères - France
†Presently with Aluminium Dunkerque, ZIP Ouest,
BP81 59279 Loon Plage - France
**Pechiney Centre de Recherches de Voreppe, 725 rue Aristide Berges,
BP27 38341 Voreppe - France

Abstract

A real-time radioscopic visualization technique was used to observe the shape and motion of argon bubbles in liquid aluminum. The images provided by a X-Ray generator on a radiographic screen were recorded and treated to extract the width and velocity of the bubbles. The treatment was validated by observations, at room temperature, of hollow spheres machined in a rotating aluminum block. The size and velocity of bubbles were measured in a parallelipipedic graphite crucible where the bubbles could flow up without interaction with the crucible walls.

Introduction

In liquid metal processing, gas bubbling is commonly used for metal stirring in ladles or for degassing. Therefore it is crucial for any improvements of these processes to better describe the bubble emission, to measure the bubbles size and velocity and to check that the predictions based on water models are valid for liquid metals. Many attempts have been made to characterize the bubbles behavior in liquid metals and compare it to what is well known for transparent liquids.

These attempts may be divided in two kind of techniques: the invasive ones, that can disturb the fluid flow and the bubble shape, and the non-invasive ones.

For the first a very interesting study has been done by Iguchi et al [1, 2, 3] who used an electroresistive probe to study gas bubbling in liquid steel at 1600°C. However it can always be suspected that the presence of a solid probe across the path of the bubbles distorted the measured characteristics, specially the bubble shape, due to triple line attachment onto the probe itself.

For the second a simple characterization technique that has been widely used consist in recording the noise created in the nozzle by the bubble detaching as Irons & Guthrie did with steels[4]. This technique gives the emission frequency of the bubbles, from which the bubble volume can be deduced for a known flow rate. The noise of the bursting bubbles at the metal surface was also used by Fu & Evans for aluminum [5] to determine the mean velocity between the emission point and the surface of the bath.

The advantage of using X-Rays cinematography, with respect to the previously presented techniques, is to also give a detailed view of the bubble shape and behavior, the local velocity and the trajectories in stirred metals. Zhang & Fruehan [6] used it to visualize slag foaming in direct steelmaking. Davis, Irons & Guthrie [7] applied it to the nucleation of gas bubbles in In-Ga alloys. Bubble behavior at a slag/steel interface was also looked at by Chevrier & Cramb [8]. In all these cases the equipment did not allow experiments with bath wider than a few centimeters, by lack of transparency of the liquid medium. Therefore it has not been possible to look at bubble trajectories or velocity in a free flow, far enough from the container walls.

In the present work aluminum bath were placed in a parallelipipedic graphite crucible of internal size: 10 cm along the X-ray path, 12 cm wide and 30 cm high. This gave the extra advantage of a free flow of the bubbles and allowed a non-perturbing characterization of shapes, motions and flow regimes of argon in liquid aluminum, at about 720°C, and in absence of mechanical stirring.

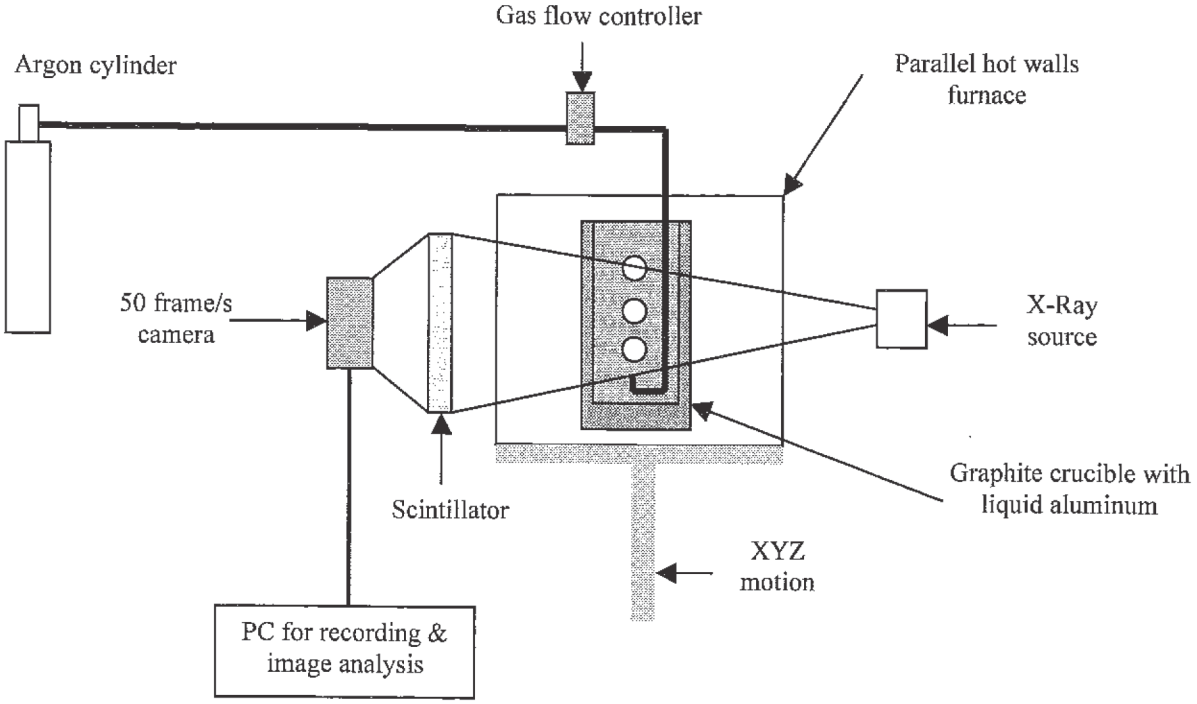

Figure 1: Schematic representation of the radiographic equipment for bubbles observation through 10cm of liquid aluminum.

Apparatus

A schema of the equipment is presented in Fig.1.
The X-rays were emitted by a tunable 0-160 kV, 0-20 mA Phillips generator. The images were formed on a radiologic scintillator (Trigicon) and recorded by a video camera at 50 Hz (one frame every 20 ms). Each frame was recorded on a computer memory.
The parallelepipedic furnace was heated by two electrical resistance on the two flat walls parallel to the X-ray beam. The amount of material on the X-rays path was minimized to avoid absorption and formation of granular contrast that would impede observations of details. Only two thin alumina wool walls were used at the ends of the furnace on the X-Ray path. The metal was placed in a parallelepipedic graphite crucible with 1 cm thick walls on the X-ray path. With this assembly observation of 10 cm thick aluminum bath was easy. The parallelepiped shape avoided the presence of absorption gradients on the background.
The furnace could be moved in three directions during the X-ray observation to center the pictures on the various fields of interest: the bubble emitter, the free flow of the bubbles, the surface of the metal bath.
The bubbles were generated by J shaped tubing with a nozzle holder at its tip facing upward. Three types of bubble emitters could be fixed on this holder, as shown in Fig.2, in order to provide various orifice size and material. The nozzle holder was made of graphite or of stainless steel lined with an aluminum resistant paste. Different type of material, shapes and size could be used with the same type of nozzle holder.
The argon flow was measured by a mass flowmeter. Between the mass flowmeter and the bubble emitter the argon passed through tubing of various length and volume capacity.

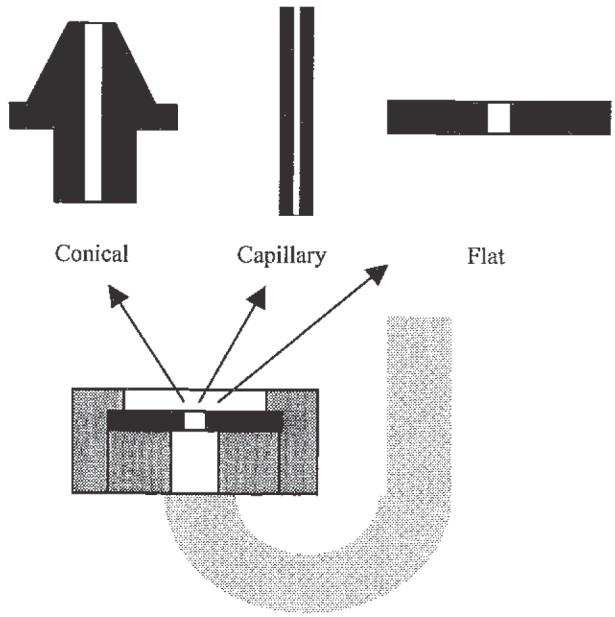

Nozzle holder with its J shaped feeding tubing

Figure 2: Three type of nozzle were used, on the same nozzle holder, to generate bubbles.

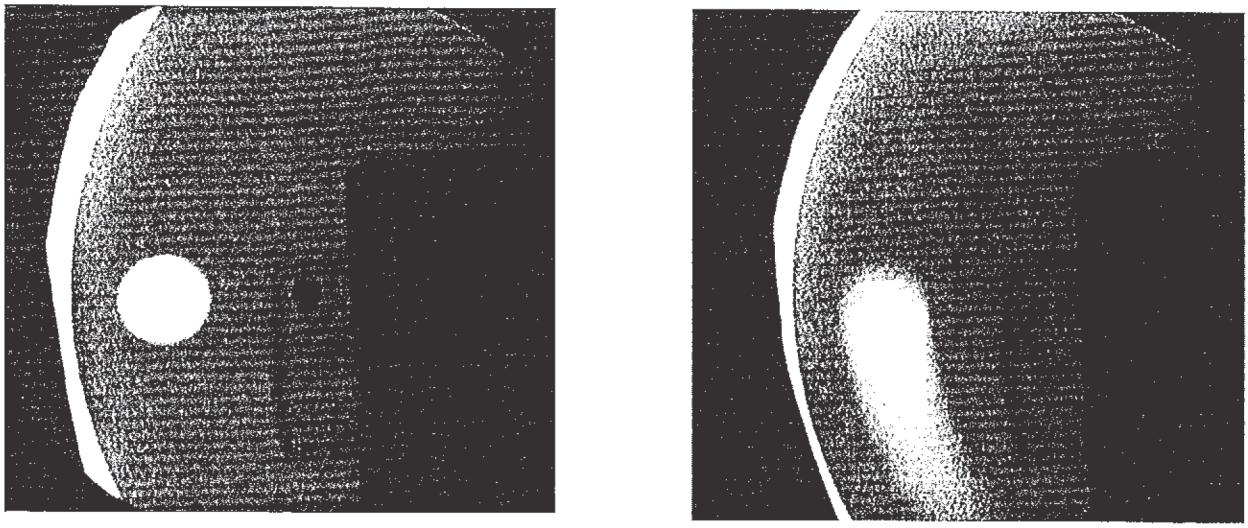

Figure 3: X-ray images of a 20mm diameter hollow sphere machined in an aluminum block, at rest on the left and rotating on the right (the center of the sphere has a linear velocity of about 0.5m/s). The tail is due to the remanence of the scintillator.

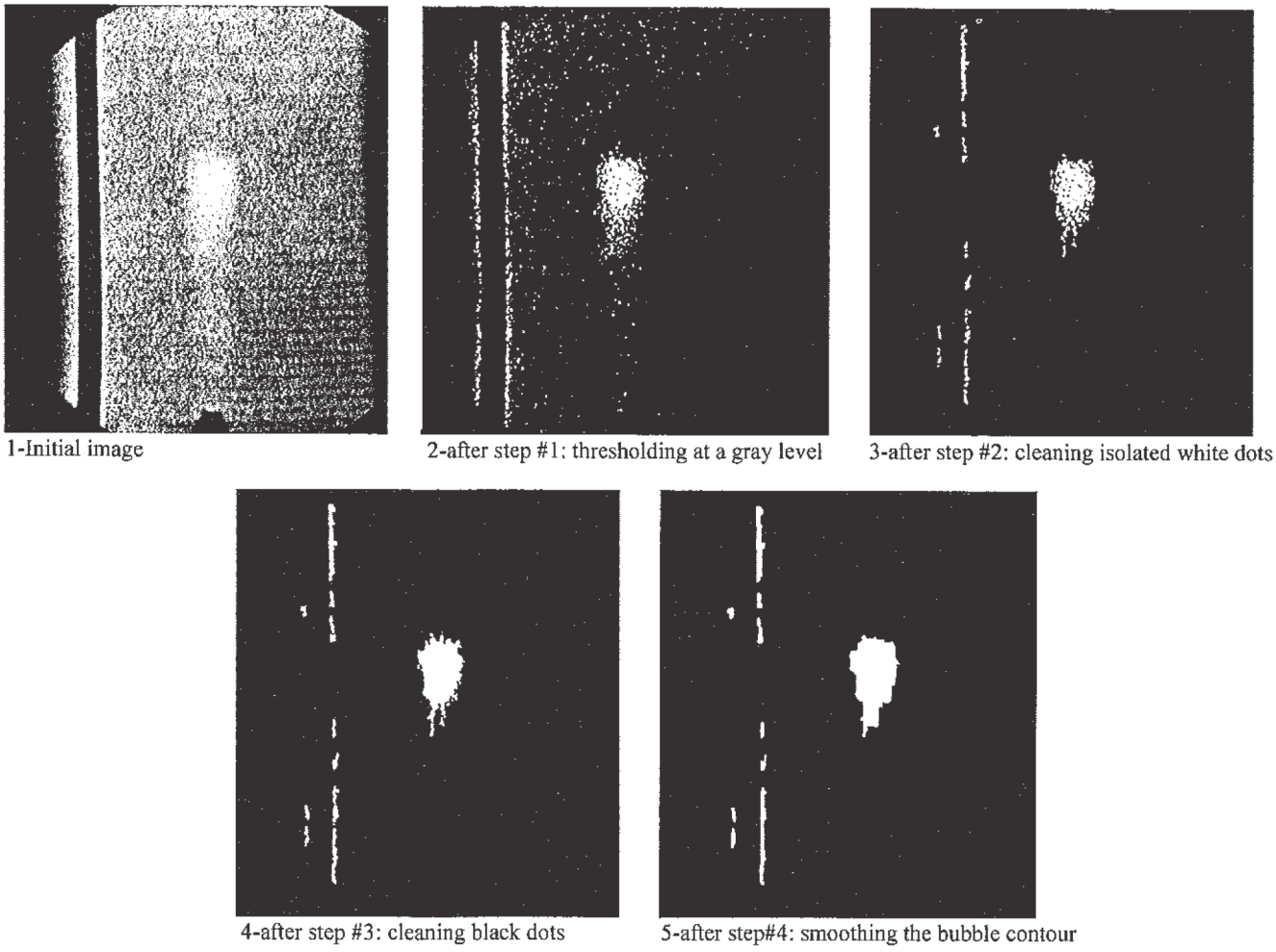

Figure 4: Image treatment in four steps to get a binary image of the bubble on which measurements can be made.

Calibration.

A calibration was necessary to carry out measurements on bubbles because their contour was always fuzzy and because a tail appeared on moving objects due to the remanence time of the scintillator. For this, hollow spheres (diameters 10.3, 16, 20, 30 mm) were machined in an 50 mm thick aluminum disc that could rotates at a given speed giving sphere center velocity from 0.50 to 1.70 m/s. The images obtained during such « cold » calibration runs were treated (Aphelion 2.2 software) in such a way that the treatment parameters led to a reproducible size measurement of the hollow spheres. An example of a static and a dynamic image of a 20 mm diameter hollow sphere is given in Fig.3.

The treatment consisted first in a conversion to a binary image of a 664*664 pixels (the size of one pixel is 0.181mm on the scintillator) with a threshold at a level of gray chosen on the edge of the background noise. Second, the noise outside the bubble (black field) is cleaned by a conditional opening eliminating small objects. Third, the background inside the « bubble » is cleaned, also by conditional opening. Fourth the contour of the bubble is smoothed. The effects of these operations are presented in Fig.4 for a gas bubble in liquid aluminum. The width of the bubble is then measured along the direction perpendicular to the trajectory. This technique allowed a precision of about 2mm on the bubble diameter, assimilated to the bubble width. The precision on the position of the center of a bubble, which was assumed spherical, is better (± 1 mm). For this measurement two frames were selected with the hollow sphere in two positions as apart as possible, i.e at a distance of about 400 pixels or 70 mm. However, although the position change between two successive frames was used to determine the bubble velocity, the accuracy of this measurement was limited by a ±3% uncertainty on the rotation speed measurements during the cold calibration

Despite this good precision small bubbles cannot be detected with this treatment. The practical limit was found to be about 8mm in diameter which is not a limiting value because the bubbles diameter are usually larger in standard processes in use for aluminum treatments.
The furnace was situated close to the scintillator and far from the X-ray source. The resulting magnification factor was only 1.07 one pixel on the 664*664 image represented a spot of 0.169mm in the center of the crucible, each frame covered a 112mm square.

Bubble nucleation

It is well known that the shape and anchorage position of a bubble nucleus primarily depends on the wettability of the nozzle material by aluminum. An example is given in Fig.5 for a flat nozzle with a 0.5 mm hole. With a plate made of a material wetted by Al (such as Ti for instance), the bubble nucleus is anchored on the inner edge of the hole and the diameter of the released bubble is about 12 ±1 mm. With a plate made of a non-wetted material (such as graphite for instance), the nucleus is anchored on the outer rim of the steel holder, giving 28±5 mm bubbles. This illustrates the fact that the bubble size depends on the hole diameter with material wetted by Al but not with non-wetted materials of large size.
However when the gas comes from a small device, such as a capillary, the size of the bubble tends to be define by the outer diameter of the device. It was observed that the triple line of the nucleus, material/gas/Al, tends to go down along the capillary until it reaches a roughness that anchors it, for a wetted and non-wetted material (steel or alumina) as well. This may be due to the fact that the inner diameter of the hole (0.2/0.3 mm) or the outer rim diameter (about 1 mm) were too small to allow a nucleus to form with a diameter large enough to allow the buoyancy to release a bubble. With such capillaries the size of the bubbles were about 10 mm.
With a gas film on the bottom of a graphite crucibles (Fig.6) the size of bubbles is larger and their diameter is not dependent on the size of the surface covered by the film. Nucleation does not take place in a well defined position

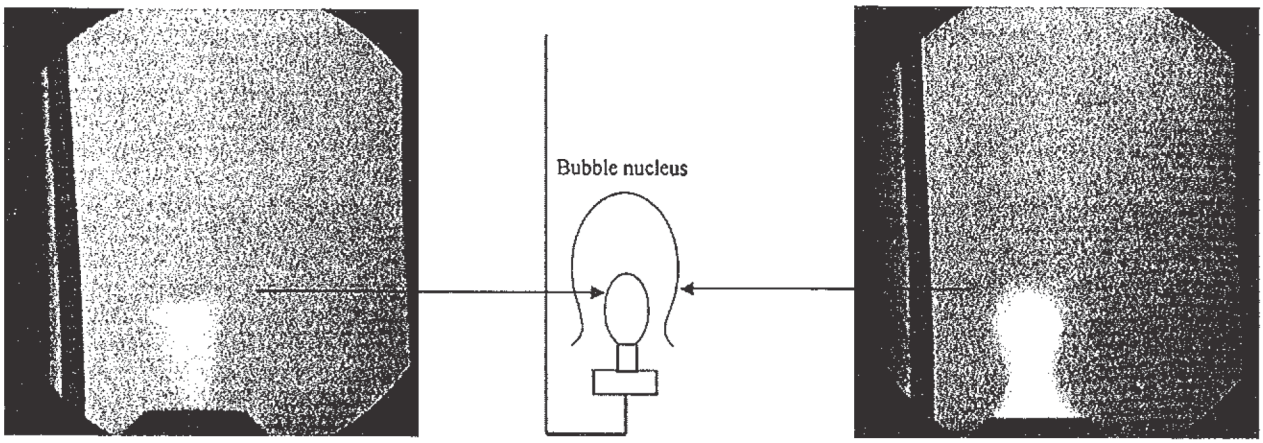

Figure 5: The bubble nucleus is anchored on the orifice inner edge with a wetted flat nozzle (left) and on the outer diameter with a non-wetted flat nozzle of the same size. The central schema illustrates this well known behavior due to wetting properties of liquids.

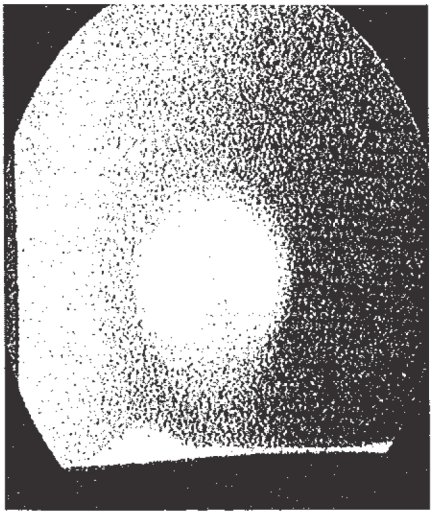

Figure 6: Large bubble (diameter about 30mm) released by a gas film on the bottom of a graphite crucible. A new instability grows on the left of the bubble.

Free bubble behavior

Three type of bubble were observed. The small bubbles (diameter of about 10mm) were spherical. The medium bubbles (diameter of about 20mm) produced on flat nozzles were ellipsoidal and wobbled all along their trajectory up. Some very large bubbles (40 mm), generated on flat surfaces covered by a gas film were spherical caps. The bubble velocity was about 0.4 m/s almost independent of the bubble size.

Following Clift et al.[9] this behavior is characterized by three dimensionless numbers:

- the Morton number, independent of bubble size and equal to 10^{-13} in the present case: $M = (g\mu^4\Delta\rho)/(\rho^2\sigma^3)$
- the Reynolds number $Re = \rho dU/\mu$
- the Eotvos number $Eo = g\Delta\rho d^2/\sigma$

where d is the bubble diameter, g the gravity, U the bubble velocity, σ the surface tension of Al, μ the metal viscosity, ρ the metal mass per unit volume and $\Delta\rho$ the difference of this mass between the metal and the gas.

According to Clift the transition between wobbling bubbles and spherical caps takes place at Eo~40. In the present case this transition occurred at Eo~30 to 40 in good agreement with the general trend. The transition between spherical bubbles and wobbling bubbles is expected at Eo~0.3 but in the present experiments it was found to occur at Eo>3, i.e. an order of magnitude higher.

For the same hole diameter a flat nozzle produces larger bubbles than a conical nozzle. This is associated with a different liquid motion at the bubble detachment as shown in Fig.7. The constriction of the nucleus implies a liquid flow parallel to the nozzle upper surface on much larger distance for a flat nozzle than for a conical one. The time necessary for the constriction is thus larger, even if the material is wetted by Al, allowing more gas to enter the nucleus before detachment of the bubble.

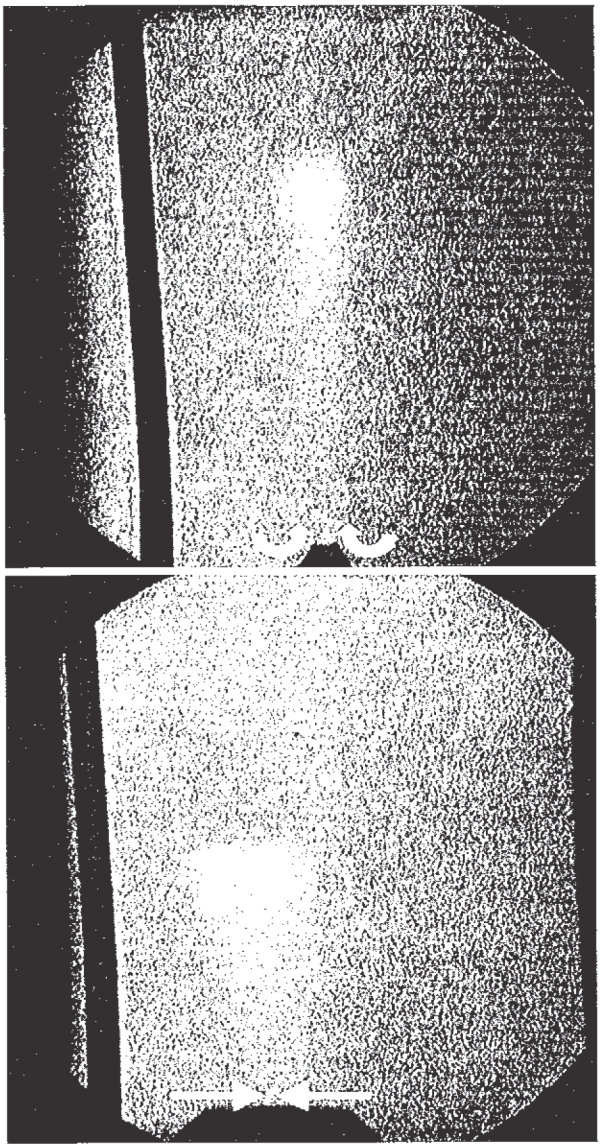

Figure 7: Comparison of two bubbles emitted by a wetted nozzle with a 3mm diameter orifice at the same flow rate. Arrows illustrate the fluid motion at the bubble detachment on a conical nozzle (upper) and a flat nozzle (lower).

The bubbles tend to form a train in unstirred aluminum bath. These train of bubble reach the surface at a point where it forms a bump due to the ascending column of liquid driven upward by the bubbles, as shown in Fig.8. No bubble coalescence has been observed in the trains nor at the surface. Coalescence occured only at the emitter at the bubble release.

The bubble velocity in these bubble trains was independent of the bubble size and the nozzle shape. It was almost independent of the gas flow rate as shown in Fig.9. However, for sake of simplification we may admit that the velocity was about 37 cm/s for flow rates below 300 stdd cc/min and about 49 cm/s for flow rates in excess of this threshold. The mean standard deviation for velocity measurements was ±8 cm/s for 10 measurements. The same bubble size could be obtained with flat or conical nozzles with orifices or various size.

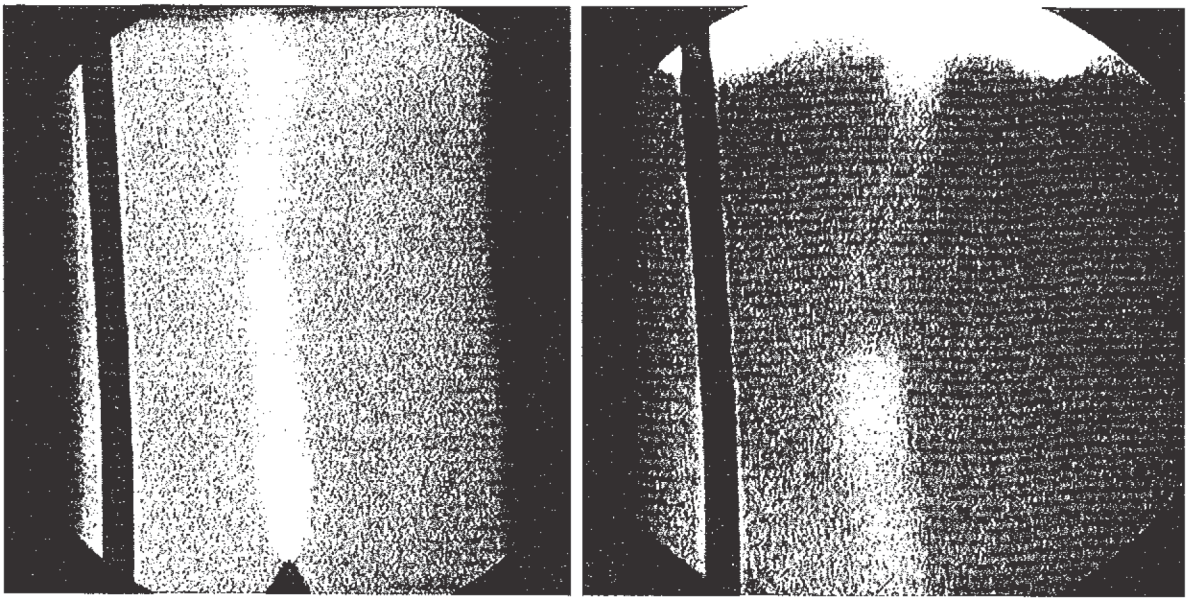

Figure 8: Visualization of a bubble train above the emitter (left) and at its emergence on the free surface (right) with formation of a bump.

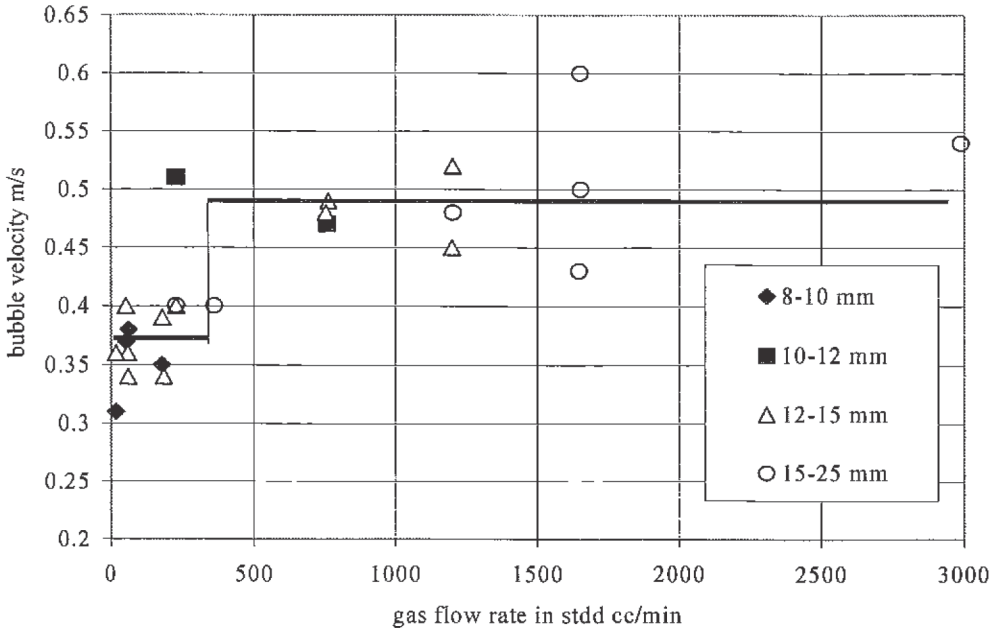

Figure 9: Bubble velocity in bubble trains versus the gas flow rate, for a single nozzle. Four classes of bubble size are distinguished to show that velocity depends mainly on the flow rate and not on the bubble diameter or the nozzle shape (flat or conical). The mean standard deviation for the bubble velocity is about 0.08 m/s.

Bubble size and capacitance

As already known the bubble diameter for a given nature and geometry of the nozzle depends on the capacitance of the gas line upstream the nozzle orifice. The capacitance is defined as the ratio of excess volume in the line to the bubble volume: (line volume - bubble volume)/bubble volume. This behavior has been checked with line volumes of 8, 30 and 1000 cc. The results are reported in Fig.10 with literature data from liquid steel and mercury. The bubble diameter is plotted versus the capacitance of the gas line. The results are very similar to what has been obtained previously in liquid metals, with a value of capacitance of about 3 for the threshold giving the limit of influence of capacitance on bubble size.

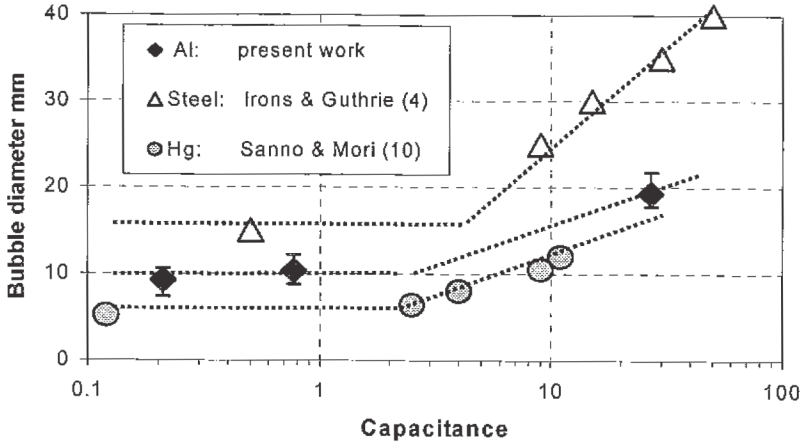

Figure 10: Bubble size versus gas line capacitance showing that the capacitance begins to influence the bubble diameter when it is in excess of about 3 whatever the temperature and the nature of the liquid metal.

Concluding remarks

A simple radiographic technique, on a standard non-destructive testing facility, has been used to study the behavior of bubbles moving freely in liquid aluminum. A calibration by cold runs was used to measure the bubble size and velocity on the frames recorded at a rate of 50 Hz. An image treatment was necessary to eliminate the effect of the blur resulting from the effect of motion on the fluoroscopic screen.

These measurements were associated with visual information on the shapes of the bubble and of the bubble nuclei. The free flow behavior of isolated bubbles or bubble trains has been observed in non-stirred aluminum.

It allowed confirming well-known behaviors:

- the bubble nucleus is anchored on the inner diameter of the orifice for material wetted by liquid aluminum and on the outer diameter of the nozzle for non-wetted material.
- for capillaries (diameter less than 1 mm)., wetted or non-wetted, the bubble nucleus is anchored outside the tubing
- the nozzle shape at the orifice has an influence on the released bubble size due to metal draining, the longer the draining the larger the bubble.
- the gas capacitance upstream the orifice has an influence on bubble size when it is in excess of about 3, the larger the capacitance the larger the bubble.
- for isolated bubbles the transition between wobbling bubbles and spherical caps takes place at Eo≈40.
- the isolated bubbles velocity is about 0.35 m/s

It allowed to observed less obvious behaviors:

- wobbling bubbles were seen to appear at Eo>3 instead of the expected value of 0.3.
- bubble velocity in continuous bubble trains was found to be about 0.5 m/s regardless of their diameter.
- continuous bubble trains appeared at a gas flow rate of about 300 standard cubic centimeters per nozzle, in absence of metal stirring.
- No bubble coalescence has been observed in the bubble trains, the formation of double bubbles was only observed at the nozzle after the bubble release.
- the bubbles seemed to cross the free surface of the metal bath without accumulation effect at the center of a bump due to the ascending metal flow

Acknowledgments

This work has been carried out with the financial support of the following French public organizations: Région Rhône-Alpes, CNRS (CPR "Qualité du métal liquide et recyclage") and Ministry of National Education.

References

1. M.Iguchi, H.Kawabata, K.Nakajima, Z-I. Morita "Measurements of bubbles characteristics in a molten iron bath at 1600°C using an electroresistive probe," Met Trans B, vol 26B, (1995), 67-74
2. M.Iguchi, T.Nakatami, H.Kawabata, "Development of multineedle electroresistive probe for measuring bubble characteristics in molten metal bath," Met Trans B, vol 2B, (1997), 409-416.
3. M.Iguchi, T.Nakatami, "The shape of bubbles rising near the nozzle exit in molten bath," Met Trans B, vol 28B, (1997), 417-423.
4. G.A.Irons, R.I.L. Guthrie, "Bubble formation at nozzle in pig iron," Met Trans B, vol 9B, (1978), 101-110
5. Q.Fu, G.Evans, "Kinetics of magnesium removal from aluminum alloys by chlorine fluxing", Light Metals, (1997), 865-870
6. Y.Zhang, R.J.Fruehan, "Effect of the bubble size and chemical reactions on slag foaming", Met Trans B, vol.26B, (1995), 803-812
7. K.G.Davis, G.A.Irons, R.I.L. Guthrie, "X-ray cinematography observations of gas injection into liquid metals", Met Trans B, vol.9B, (1978), 721-722.
8. V.F.Chevrier & A.W.Cramb, "X-Ray fluoroscopic observations of bubble formation and separation at a metal-slag interface", Met Trans B, vol.31B, (2000), 537-540
9. R.Clift, J.R.Grace, M.E.Weber, in Bubbles Drops and Particles, (Academic Press, N-Y, 1978), 27.
10. M.Sanno, K.Mori, "Bubble formation from single nozzles in liquid metals", Trans J.I.M., vol 17, (1976), 344-352.